DESIGN OF AN AERODYNAMIC MEASUREMENT SYSTEM FOR UNMANNED AERIAL VEHICLE AIRFOILS

L. Velázquez-Araque[1] and J. Nožička[1]

[1] Department of Fluid Dynamics and Power Engineering, Faculty of Mechanical Engineering
Czech Technical University in Prague, Czech Republic

ABSTRACT

This paper presents the design and validation of a measurement system for aerodynamic characteristics of unmanned aerial vehicles. An aerodynamic balance was designed in order to measure the lift, drag forces and pitching moment for different airfoils. During the design process, several aspects were analyzed in order to produce an efficient design, for instance the range of changes of the angle of attack with and a small increment and the versatility of being adapted to different type of airfoils, since it is a wire balance it was aligned and calibrated as well. Wind tunnel tests of a two dimensional NACA four digits family airfoil and four different modifications of this airfoil were performed to validate the aerodynamic measurement system. The modification of this airfoil was made in order to create a blowing outlet with the shape of a step on the suction surface. Therefore, four different locations along the cord line for this blowing outlet were analyzed. This analysis involved the aerodynamic performance which meant obtaining lift, drag and pitching moment coefficients curves as a function of the angle of attack experimentally for the situation where the engine of the aerial vehicle is turned off, called the no blowing condition, by means of wind tunnel tests. The experiments were performed in a closed circuit wind tunnel with an open test section. Finally, results of the wind tunnel tests were compared with numerical results obtained by means of computational fluid dynamics as well as with other experimental references and found to be in good agreement.

INTRODUCTION

According to the evolution of unmanned aerial vehicles, commonly referred to as UAVs, several investments have been increasing every year, especially in the field of aerodynamic characteristics which can be obtained through wind tunnel tests.

In the Laboratory of Fluid Mechanics at the Czech Technical University in Prague, particularly in the branch of aerodynamics, a measurement system to get aerodynamic data is needed. Based in the methodology of A. Suhariyomo et al. and J. Barlow et al., this paper presents the design of an aerodynamic characteristic measurement system for UAVs which consists mainly in the design of an aerodynamic wire balance. The balance and the wind tunnel complete the data acquisition system which is verified to assess whether the measurement system is suitable for measuring the aerodynamic performance of different airfoils. The verification was performed with a two dimensional NACA 2415 airfoil, comparing it with reference results in [1,6] and [7], measuring lift, drag forces and pitching moment. In order to go further in the validation of the measuring system, four modified models of this base airfoil were made and tested in the balance; the modification consisted in a step located in the suction surface of each airfoil at 30, 40, 50 and 60 percent of the cord. Lift, drag and pitching moment coefficients versus the angle of attack were obtained for all the models tested and were compared to numerical results obtained in [7]. The whole process is described in the following sections.

DESIGN OF THE BALANCE

This aerodynamic balance was designed for testing the performance of different airfoils for unmanned aerial vehicles measuring lift, drag forces and pitching moment, special attention was paid in this stage because since UAVs fly at low speeds, the magnitude of the forces will be very small, therefore important accuracy is required [5].

Description

The structure of the balance was designed according to the dimensions of the open wind tunnel test section using commercial CAD software; the selected parts for the frame were aluminum profiles due its weight and easy connectivity between the other parts as seen in Figure 1. The balance is composed of six high precision digital hanging scales with a capacity of 50N and a resolution of 0,02N located according to Figure 2.
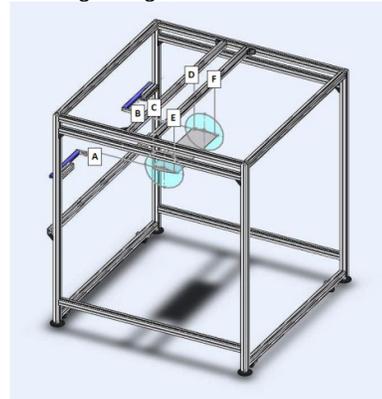

Figure 1. Structure of the aerodynamic balance.

Six forces are measured in scales A, B, C, D, E and F. The wires attached to A and B are parallel to the incoming velocity vector and define a plane which is taken as a reference plane for the balance (x-y plane), these wires point in the x direction.

Figure 2. Location of scales in the aerodynamic balance.

The wires attached to C and D are in a plane that is perpendicular to the x-y plane, which is designate the y–z plane. Wires containing A and C are attached to a common point on the left side of the wing. Wires

containing B and D are attached to a common point on the right side of the wing. Finally wires attached to E and F are parallel to those ones attached to C and D.

The airfoil is attached to two endplates of transparent polycarbonate as shown in Figure 3, these endplates have the main function of reducing considerably the strength of the tip vortices and the induced drag by blocking the leakage around the wing tips [2].

Figure 3. Endplate detail

The balance can produce angle of attack (AOA) changes from 0 to 16 degrees manually with the smallest increment of 2 degrees.

MEASUREMENT SYSTEM APPARATUS

The measurement system includes three components, a low speed wind tunnel system, the aerodynamic balance and data processing software.

Wind Tunnel System

The closed-circuit wind tunnel has an open test section of 750 x 550 mm cross section. It is assembled from straight parts of a closed-return passage with rectangular cross section, elbows with corner-vanes, a rectangular settling chamber and a nozzle. The honeycomb and two screens are placed in a closed-return passage as shown in Figure 4. The maximum air velocity of 17 m/s can be obtained in the test section. A 55 kW three-phase induction motor and a frequency changer are coupled with fan. The wind tunnel has a turbulence intensity at a velocity of 7,5m/s of 1,3% [11]. The flow velocity was measured directly with an anemometer vane type.
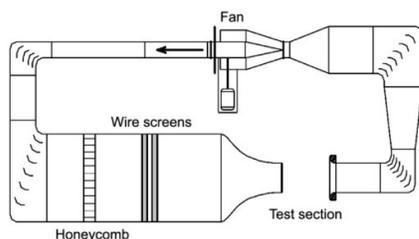

Figure 4. Low speed wind tunnel.

Data acquisition and processing

The procedure for the acquisition and processing the data is in agreement to the procedure for wire balances, attaching the model in an inverted position (upside down) so that aerodynamic lift added to the weight to prevent unloading the wires as the resulting tension can never be allowed to diminish to zero as reviewed in [6].

Since the horizontal wires A and B cannot transmit bending, the vertical force perpendicular to the flow velocity vector, the lift, is obtained from the sum of the forces in the vertical wires:

$$F_L = C + D + E + F \qquad (1)$$

The drag is the sum of the forces in the two horizontal wires parallel to the direction of the flow velocity:

$$F_D = A + B \qquad (2)$$

The pitching moment is about the y axis is given by:

$$M_P = (E + F) \times b \qquad (3)$$

where b is the distance between the lines containing C, D and E, F.

All obtained data is collected manually and then processed using calculation software. Then, the general equations to calculate lift, drag and pitching moment coefficients were used as follow:

$$C_D = \frac{F_D}{\frac{1}{2}\rho V^2 A} \qquad (4)$$

$$C_L = \frac{F_L}{\frac{1}{2}\rho V^2 A} \qquad (5)$$

$$C_M = \frac{M_P}{\frac{1}{2}\rho V^2 AC} \qquad (6)$$

Calibration of the measurement system

Since the lift is the largest force by far in a typical aircraft complete model wind tunnel work, extreme care must be taken to ensure that it is orthogonal to the other components [9]. Therefore, the most precise perpendicularity between the wires had to be maintained; otherwise some component of the drag could appear improperly in the lift and vice versa. Concerning the scales, a calibration testing process with low weights from 0,30N to 1,00N was held to observe if each scale was, in fact, measuring what it indicated. (Table 1). The resultant deviation of the scales was ± 0,02N. This possible measurement error for the used conditions represents approximately a change of 0,005 in the computed coefficients.

WIND TUNNEL TESTS

Description

In order to validate the measurement system, low Reynolds number wind tunnel tests on a two dimensional NACA airfoil and four modified models of this one were performed, these results were compared to reference experimental and numerical data.

A NACA 2415 airfoil, which has become increasingly popular on ¼ scale pylon racers [1], was tested as seen in Figure 5. The coordinates were obtained from [4].
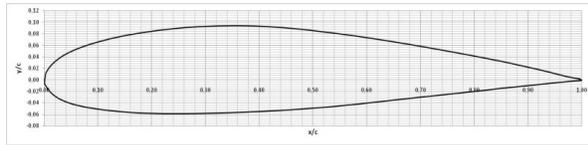
Figure 5. NACA 2415 airfoil

The modification is based mainly on the creation of an abrupt step on the suction side of the original NACA 2415 airfoil. This step simulates a blowing propulsive outlet of the wing in normal flight conditions. The height of the step must be long enough in such a way that does not risk the stability of the structure of the wing model, for that reason the height of the step was defined as one third of the maximum thickness of the original airfoil which means 5 per cent of the chord. It is important to mention that the height of the step was kept constant to focus mainly on the influence of the location of the step along the chord line.

Four different configurations where designed which involved the location of the step at different strategical points chordwise. These points are:

- At the location of the maximum thickness: 30% of the chord (2415-3).
- At the location of the maximum camber: 40% of the chord (2415-4).
- Before the transition point (at 0 AOA): 50% of the chord (2415-5).
- Passed the transition point (at 0 AOA): 60% of the chord (2415-6).

Therefore, four models were built and also the original NACA 2415. Following the NACA numbering system, it was proceeded to assign an additional digit which indicates the position of the step chordwise in tenths of the chord.

The following equations were developed to obtain the ordinates passed the step, since the abscises and ordinates of the original airfoil are given with respect to the origin (0,0),

for $x=x_s$:

$$y_{Um_{x=x_S}} = [y_U]_{x=x_S} - h_S \qquad (7)$$

for $x>x_s$:

$$y_{Um_{x>x_S}} = \left[\frac{y_U - h_S}{y_U}\right]_{x=x_S} \cdot [y_U]_{x>x_S} \qquad (8)$$

where:

- y_{Um} is the modified ordinate of the upper surface.
- x_s is the abscise of the step.
- h_s is the height of the step.

In Figure 6 it is possible to see all the parameters involved in the modification of the base airfoil, in this case where the step is located at the maximum thickness point.
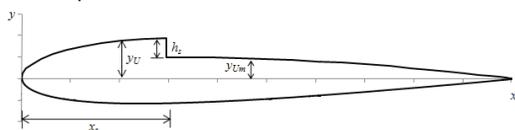

Figure 6. Parameters involved in the modification of the base airfoil

The resulting airfoils after the corresponding modifications are illustrated in Figure 7 a,b,c,d.
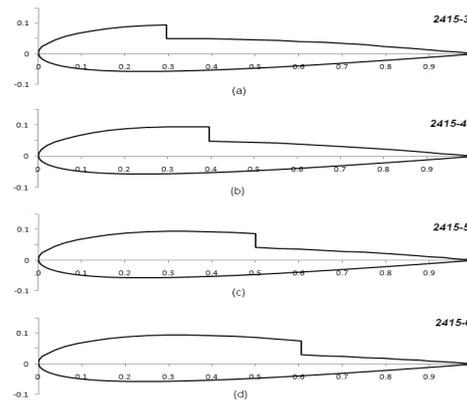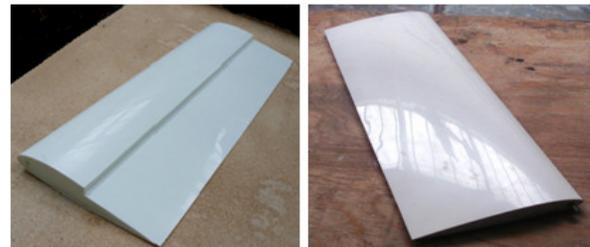

Figure 7. Airfoils developed for testing (a) 2415-3, (b) 2415-4, (c) 2415-5, (c) 2415-6.

The NACA 2415 and all developed airfoil models built for testing (Figure 7 a,b,c,d) have a chord length of 200 mm and a span of 600 mm, which means an aspect ratio of 3. The body of the models was made of expanded polystyrene foam (EPS) and coated with a layer of solid polystyrene as shown in Figure 8 a,b.

(a) 2415-5   (b) NACA 2415
Figure 8 a,b. Airfoil models for testing.

In order to run the tests, the aerodynamic balance was fixed and aligned in the wind tunnel open test section, then the model previously attached to both endplates by means of screws and nuts was hanged in the four scales for lift which were attached to the balance structure and finally it was connected to the two drag scales forming an angle of 90 degrees. The wind tunnel tests were performed at a Reynolds number of 100000 which means a velocity of 7,7 m/s according to the climatic conditions of the measurement days. The angle of attack was set from 0 to 16 degrees with an increment of 2 degrees [8]. The experimental results are validated with numerical results which will be also described later in the following sections.

Adjustments

In order to obtain the aerodynamic forces applied only on the model, the drag of the endplates and the rod which hold the model in the model had to be obtained because it is also being measured by the drag scales, for this purpose the endplates attached

with the rod where mounted and the drag force was measured by scales A and B.

Then, the drag force of the rod was computed by means of Eq. (4) using as its drag coefficient the one obtained in reference with the corresponding Reynolds number.

RESULTS AND DISCUSSION

In the following graphs (Figures 9 and 10) the aerodynamic performance of a model of a NACA 2415 airfoil is shown, experimental and numerical data from references [1,6] and [7] respectively are also included.

In the lift coefficient graph shown in Figure 9, it can be observed that the stall region appears for an angle of attack of 16 degrees with a C_L of approximately 0,96. In this point, the measured C_L is higher that the C_L from experimental reference in [6] at Re=340000. However it is slightly lower than the reviewed in the numerical reference in [7] at Re=100000. Comparing to reference in [1] at Re=100000, all values of the measured C_L are considerably lower.
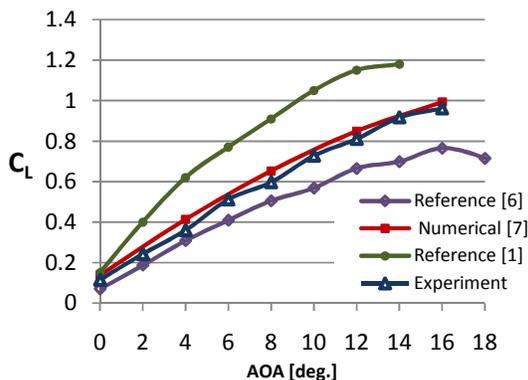

Figure 9. Lift coefficient graph of NACA 2415 airfoil.

In Figure 10 it is possible to see the drag coefficient as a function of the AOA for the NACA 2415 airfoil, the measured C_D is in very good agreement with numerical reference. Comparing to the C_D reviewed in [6], all the values are very similar but these latter ones are slightly smaller, from an AOA of 16 degrees the C_D increases considerably but this value could not be compared because as mentioned before, the highest possible AOA is 16 degrees so far. Concerning the reviewed reference in [1], all the values are considerably smaller than the measured ones and all other references. These discrepancies in drag are assumed to be primarily caused by imperfections in the airfoil construction and the inaccuracies in the experiment.

Figures 11 - 14 show C_L versus AOA, C_D versus AOA, C_L versus C_D and C_M versus AOA of four wings which have a NACA 2415 airfoil as a base shape and a step on the suction side located according to Figure 7. Each graph also presents obtained experimental results of the original NACA 2415 for further comparison. All the wings were tested at a Reynolds number of 100000.
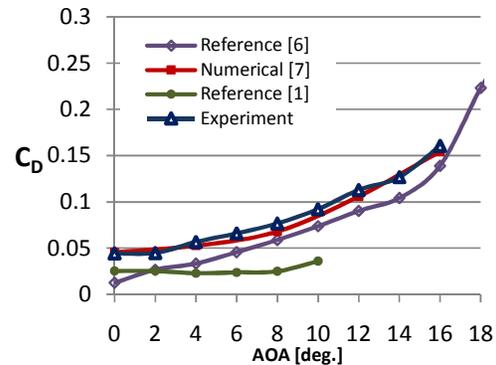

Figure 10. Drag coefficient graph of the NACA 2415 airfoil.

Concerning the lift coefficient, shown in Figure 11, it can be seen that the location of the step does not have influence on the slope of the lift curve, however as the step moves towards the trailing edge, the lift curve moves upwards, therefore this affects the values of the lift coefficient. The 2415-3 airfoil has the lowest lift for all angles of attack and its behavior is close to a symmetric airfoil (almost zero lift at zero angle of attack). The curve is linear until 14 degrees of AOA where an abrupt decrease begins which corresponds to the stall point.
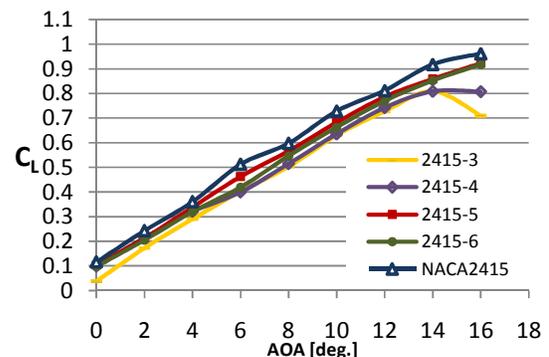

Figure 11. Experimental lift coefficient graph for all airfoils models.

The 2415-4 airfoil lift coefficient at zero angle of attack is approximately higher by 0,07 than the corresponding value for the 2415-3. The lift curve of the airfoil is not linear, at 6 degrees of AOA the curve follows the same path of the one for the 2415-3 airfoil curve until an AOA of 14 degrees where a low decrease starts. The results show that the 2415-3 and 2415-4 airfoils have approximately the same stall point at 14 degrees of AOA but after this point, the decrease in lift for 2415-3 airfoil is much more abrupt.

The lift coefficient behavior for 2415-5 and 2415-6 airfoils is very similar. The curves start at the same value of C_L, like 2415-4 airfoil but their path is approximately linear until 12 degrees of AOA where the slope begins to shrink moderately. The presence of the stall point for these curves is not shown very clear but it can be assumed that is very next to 16 degrees of AOA. The original airfoil lift curve has slightly higher values of C_L for all AOA but its behavior is almost the same; the

stall region begins after 15 degrees of AOA. These characteristics were expected since the step produces a sudden change in the pressure distribution along the upper side of the airfoils which contributes to decrease the lift.
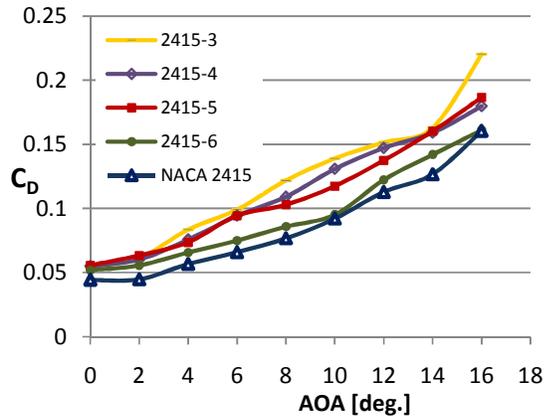

Figure 12. Experimental drag coefficient graph for all airfoils models.

In Figure 12 above it is possible to see the drag coefficient versus the AOA for all the models tested. All of the modified airfoils reached approximately the same value of drag coefficient at zero angle of attack. The drag coefficient of the original airfoil value is about 0,01 lower. A similar behavior of all drag curves is seen at 2 degrees of AOA.

The 2415-3, 2415-4 and 2415-5 airfoils presented similar drag characteristics for low AOA, specifically until 6 degrees, after this angle the values of C_D are different until 14 degrees of AOA where the three curves present almost the same value of C_D. Also, between 6 and 14 degrees of AOA the 2415-3 airfoil presents high values of C_D followed by the 2415-4 and 2415-5. After 14 degrees of AOA, the drag for 2415-4 and 2415-5 is similar and the drag of 2415-3 airfoil showed a substantial increment.

The 2415-6 airfoil drag curve is similar to the original NACA 2415 airfoil curve; there is only certain shift at 10 degrees of AOA where both drag coefficient values are almost the same. From this AOA the drag of 2415-6 increases again until 16 degrees of AOA where the C_D value of both airfoils equals. It is clear that the 2415-6 airfoil presented the best drag performance among all modified airfoils tested.

The polar diagram shows a lot of information in a very compact format; therefore it is always considered the most important part of the results [10]. In Figure 13 it is possible to see the polar curves of all airfoils tested. One of the important points in this diagram is the optimum glide ratio (OGR) which is obtained drawing a line from the origin (C_L=0, C_D=0) tangentially to each curve according to the diagram the results are:

- NACA 2415: OGR=7,778 at 9 degrees of AOA.
- 2415-6: OGR=6,947 at 10 degrees of AOA.
- 2415-5: OGR=6,0 at 10 degrees of AOA.
- 2415-4: OGR=5,161 at 13 degrees of AOA.
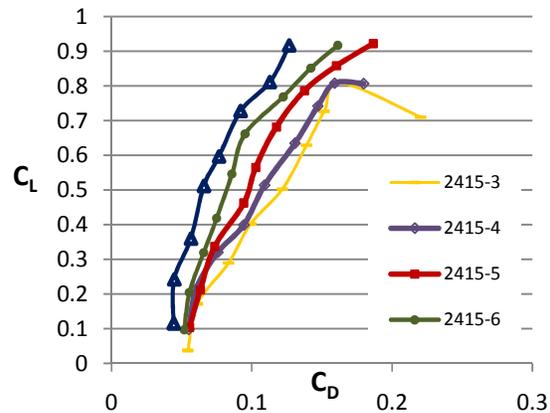- 2415-3: OGR=5,142 at 13 degrees of AOA.

Figure 13. Experimental polar graph for all airfoils models tested.

According to this the curves can be divided in two groups. In the first group (2415-3 and 2415-4 airfoils) the stall points were achieved at 14 of AOA and the curves are convex between 4 and 14 degrees of AOA. In the second group (2415-5 and 2415-6 airfoils) the curves are convex in a very small range between 4 and 8 degrees of AOA and the stall point was not achieved at the measurable scale. The original airfoil polar is concave in almost the whole range of AOA. This diagram also can show a general idea of the aerodynamic performance of airfoils and it is possible to see that while the location of the step chordwise moves to the trailing edge, the aerodynamic performance of the airfoil tested increases.

The pitching moment coefficient was obtained by means of Eq. (6) and it is computed with respect to the leading edge according to the aerodynamic balance as shown in Figure 14. In this chart it is possible to observe that the differences between the NACA 2415, 2415-6 and 2415-5 airfoils are minimal. The 2415-4 airfoil presents a lower moment until 4 degrees of AOA and after this point the moment values are similar to 2415-5, 2415-6 and NACA 2415 airfoils. The 2415-3 airfoil presented a lower pitching moment along all AOA.
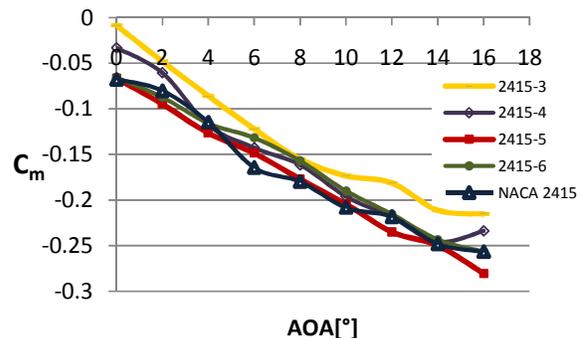

Figure 14. Experimental pitching moment coefficient at the leading edge for all airfoils models tested.

In Figure 15 it is possible to see the pitching moment coefficient with respect to a point located at 25% of the chord from the leading edge, this point is usually approximated as the aerodynamic center. This

moment was computed by means of the following equation:

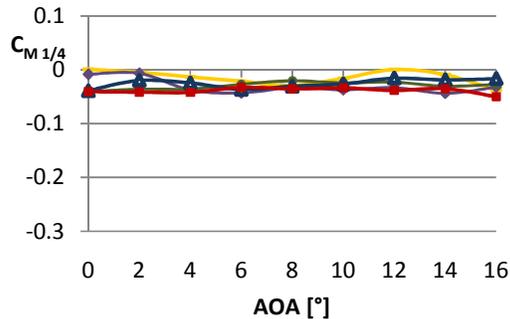$$(C_m)_{1/4} = C_m + \frac{1}{4}C_L \qquad (9)$$

Figure 15. Experimental pitching moment coefficient at 25% of the chord for all airfoils models tested.

In theory, the aerodynamic center is the point at which the pitching moment coefficient for the airfoil does not vary with the angle of attack [10]. It can be seen also in Figure 15 that the pitching moment coefficient for all models tested had very small differences with respect to the AOA, it was negative which indicates a pitch down tendency and the values were in a range between 0,00 and -0,04.

In Figure 16 it is possible to observe the lift to drag ratio C_L/C_D versus AOA, this diagram is used to see the performance of all airfoils tested and along all AOA, in this manner it is clear that all modified profiles reached their maximum C_L/C_D in a smaller range angle of attack comparing to the NACA 2415 airfoil, this one presents a maximum C_L/C_D of 8 for a range between 6 and 10 degrees of AOA.
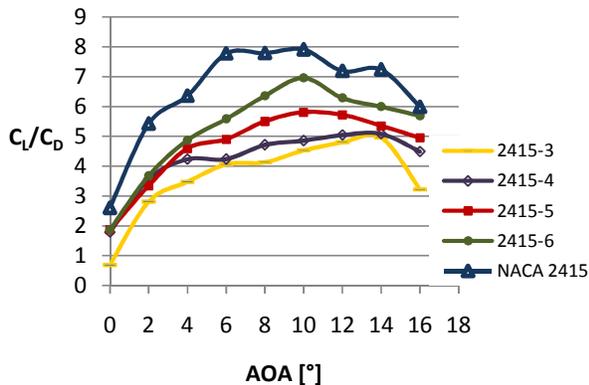

Figure16. C_L/C_D versus AOA for all airfoil models tested.

The maximum C_L/C_D for 2415-6 and 2415-5 airfoils is 7 and 6 respectively at 10 degrees of AOA. The 2415-4 and 2415-3 airfoils presented a maximum C_L/C_D of approximately 5 in a range between 10 and 14 degrees of AOA.

CONCLUSION

A measurement system for aerodynamic characteristics of unmanned aerial vehicles was designed including a low speed wind tunnel and the aerodynamic balance reviewing previous investigations. The balance was designed and built in this study. In order to validate the design a wing model of a NACA 2415 airfoil was built and tested, the results were compared to experimental and numerical reference data and found in good agreement. Then four modified airfoils were built with and tested, the results showed that the aerodynamic performance of the airfoil increases when the step moves towards the trailing edge. As further study, it is recommended to design a system which allows performing tests of these airfoils with blowing and make comparisons with results obtained in this paper. To sum up, according to the results in this research, it can be concluded that the aerodynamic measurement system is acceptable for measuring the performance for different wing models for unmanned aerial vehicles.

REFERENCES

[1] Selig M.S., Lyon C.A., Giguere P., Ninham C., Guglielmo J.J.(1996): "Summary of Low-Speed Airfoil Data", Vol. 2, Viginia Beach, SoarTech Publications.
[2] Barlow J.B., Rae W. H., Pope A.(1999): "Low-Speed Wind Tunnel Testing", 3rd ed., New York, John Wiley & Sons, Inc.
[3] Suhariyono A., Hyun Kim J., Seo Goo N, Cheol Park H., Joon Yoon K.(2005): "Design of Precision Balance and Aerodynamic Characteristic Measurement System for Micro Aerial Vehicles", Konkuk University.
[4] Abbott I.H., Von Doenhoff A.E.(1959): "Theory of Wing Sections", New York, Dover Publications Inc.
[5] Pope A.(1954): "Wind Tunnel Testing", 2nd ed., New York, John Wiley & Sons, Inc.
[6] Ghods M.(2001): "Theory of Wings and Wind Tunnel Testing of a NACA 2415 Airfoil", Technical Communication for Engineers, University of British Columbia.
[7] Velazquez L. (2010): "Development of an airfoil for an unmanned aerial vehicle with internal blowing propulsion system".PhD Thesis. CTU in Prague.
[8] Velazquez L., Nožička J.(2009): "Low Speed Wind-Tunnel Testing for an Unmanned Aerial Vehicle", Proceedings of Colloquium of Fluid Dynamics 2009, Prague, 2009.
[9] Tropea, Yarin, Foss (Eds.)(2007): "Springer Handbook of Experimental Fluid Mechanics", Springer.
[10] Clancy L.J.(1986): "Aerodynamics", Sterling Book House, Mumbai.
[11] http://profily.fs.cvut.cz/, Laboratory of Department of Fluid Dynamics and Power Engineering of the CTU. Section Airfoils and Straight Blade Cascades.